International Journal of Engineering Research and Development
e-ISSN: 2278-067X, p-ISSN: 2278-800X, www.ijerd.com
Volume 13, Issue 5 (May 2017), PP.17-28

On the Vibration Characteristicsof Electrostatically Actuated Micro\nanoResonatorsMade of Non-perfect Conductor Materials

[1]Reza Moheimani[*],[2]Abdolreza Pasharavesh, [1]Preetam C. Mohapatra
[1]*School of Mechanical and Materials Engineering, Washington State University, Pullman, WA, USA*
[2]*School of Mechanical Engineering, Sharif University of Technology, Tehran, Iran*
*Reza.moheimani@wsu.edu

Abstract:
Electrostatic actuation is one of the most prevalent methods of excitation and measurement in micron to Nano scale resonators. Heretofore, in the dynamical behavior analyses of these systems, the resonating beam has been assumed to be perfect conductor which is obviously an approximation. In this paper, effect of electrical resistivity on the vibrational response of these systems including natural frequency and damping, is investigated. The governing coupled nonlinear partial differential equations of motion are extracted and a finite element formulationby developinga new electromechanical element is presented. Calculated natural frequencies are compared with experimental measurements and a closer agreement is achieved in comparison with previousfindings. Results indicate there is a jump in frequency and damping of the system at a critical resistivity. As system size is decreased and applied voltage approaches toward pull-in voltage, electrical resistivity fully dominates the response nature of the system.

Keywords:Electrical resistivity; Electrostatic actuation; Vibration characteristics; Micro\nano resonators;

Nomenclature

b	Beam width	$\Delta\omega$	Frequency shift ratio
d_0	Initial gap	ε_0	Vacuum permittivity
E	Young's modulus of the beam	λ	Free charge per unit length
E_y	Effective Young's modulus of the beam	μ	Mass per unit length of the beam
h	Beam thickness	ν	Poisson's ratio
I_b	Moment of inertia of the cross-section	ξ	Damping ratio
l	Beam length	ρ	Electrical resistivity
N_0	Initial (residual) axial load	$\Phi(x)$	Deflection mode shape
$V(x,t)$	Voltage distribution on the beam	$\Psi(x)$	Voltage distribution mode shape
V_0	Applied voltage	ω	Natural frequency
$W(x,t)$	Beam deflection	ω_0	Natural frequency at $\rho=0$.
$W_s(x)$	Static beam deflection		

Greek symbols

I. INTRODUCTION

Micro and Nano electromechanical systems (MEMS\NEMS) technology has experienced lots of progress in recent years and has led to a revolution in production of various equipment. These systems due to their small size, light weight and low-energy consumption are extensively used as actuators, sensors and other devices.MEMS applications of an electrostatically actuated micro-beaminclude resonators, pressure sensors, accelerometers, capacitive switches, multi-electrode tunable capacitors and material property measurement among others [1-6].Electrostatically actuated Nano-beams are used in the design of NEMS applications such as Nano-tweezers and Nano scale actuators [7].

An electrostatically actuated micro\nano beam is an elastic beam suspended over a substrate actuated by applying specific voltage between the beam and substrate**.** Inresonant sensors, voltage applied across the beam is the summation of a direct current (D.C.) voltage and an alternating current (A.C.) harmonic voltage. The D.C. voltage causes a static deflection while the A.C. part forces the beam to vibrate around this static

deflection. Mostly A.C. voltage amplitude is much smaller than the D.C. voltage and the beam resonance frequencies are determined by the D.C. voltage.

Studying vibrational behavior of these systems is useful in parameter selection of the designed sensors and actuators. Vibrational characteristics of micro-beams have been generally studied assuming small vibrations around the deflected position. Ijntema and Tilmans[8] and Tilmans and Legtenberg[9] considered the static and dynamic analysis of a micro-beam under electric actuation using a linear micro-beam equation of motion. Also Nonlinear Vibrations of electrostatically actuated structures has been studied implementing different methods for solving the nonlinear equations, such as differential quadrature, finite element and homotopy methods[10]-[14].

Effect of various phenomena on the vibration of these structures is investigated in the literature. Younis has modeled microstructures considering thermoelastic damping [15]. Nayfeh and Younis also have studied the squeeze film damping effect on the vibration frequency [16]. Effect of Casimir and van der Waals forces on vibration and pull-in parameters are studied for MEMS [17]-[19] and NEMS [20], [21]. Oscillatory behavior of micro-beams considering residual stress and mid-plane stretching has been studied by R.C.Batra et al. [22] and Abdel-Rahman et al. [23]. Also the electromechanical models are improved by incorporating the effect of fringing fields, to studythe vibration of wide and narrow beams[12], [22].

It should be noted that effect of electrical resistivity of beam is not considered in any of these studies and the voltage distribution is assumed to be uniform across the beam which is true only for perfect conductors. Vibrational analysis of these electrostatically actuated beams considering electrical resistivity is very important since the range of working of micro and nanodevices is associated with the dynamic response of these structures.

In this study, effect of electrical resistivity of a Micro\Nanobeam on the vibrationresonance frequency and damping ratio is investigated. Considering different sources of nonlinearity such as electrostatic force and mid-plane stretching, thecoupled nonlinear partial differential equations which govern the motion and voltage distribution of the beam are developed. Designing a new electromechanical element, finite element method is implemented to solve the equations for the static deflection and vibrational response. To verify the model, calculated resonance frequencies are compared with the measured data for micro-beams.The dynamical behavior of the structure is investigated in different ranges of electrical resistivity, for Micro and Nano scale systems.

II. THEORY AND FORMULATION

Consider a clamped-clamped Micro\Nano beam suspended above a rigid substrate,as shown in Fig. 1. The substrate is assumed to be an ideal conductor i.e. the resistivity is considered to be negligible, consequently the voltage of the substrate is uniform, while the suspended beam is imperfect conductor with electrical resistivity $\hat{\rho}$ and voltage distribution function as$\hat{V}(x,t)$.

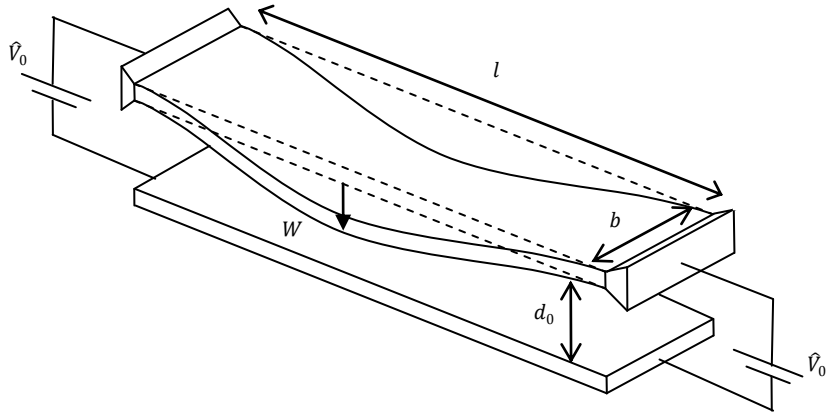

Fig. 1: Schematic view of an electrostatically actuated clamped-clamped micro\nano beam

In Fig. 1, the coordinates along the length and thickness of the beam are assumed to be in $\hat{x}$ and $\hat{z}$ directions, respectively and$\hat{W}$ is deflection in the $\hat{z}$ -direction and $\hat{t}$ is the time. The physical and geometrical properties of the beam are effective Young's modulus E_y ,mass per unit length μ , length l , width$b$ and thickness h .For a narrow beam with plane stress assumption $E_y = E$, where E is the Young'smodulus of the material, while for a wide beam implementing plane strain assumption, $E_y = E/(1-\nu^2)$, where$\nu$is Poisson's ratio [23].The

vacuum permittivity is ε_0, the moment of inertia of the cross-section about the $\hat{y}$ -axis, I_b, and the initial gap between the beam and the substrate is d_0.

Let a DC voltage $\hat{V}_0$ is applied between the clamped ends of the beam and the substrate. This voltage results in opposite electrical charges to be distributed on the beam and substrate causing an attractive force on the beam. Let the capacitor formed by the beam and substrate be divided into small capacitors with plates of length $d\hat{x}$ and width b. When the beam undergoes vibration, the gap of these capacitors varies which results the charge stored on the capacitor to be changed, causing a current in the beam in $\hat{x}$ -direction. Considering beam resistivity this current causes the voltage to vary along the beam and this voltage variation changes the force applied to the beam.

Another important parameter affecting the force between the beam and substrate is the so-called fringing field. Effect of fringing fields due to finite thickness of the beam, may be evaluated through Palmer's formulation which improvesthe capacitance estimation between a wide beam and the substrate[24]. Consider an element of beam of length $d\hat{x}$, Palmer's formula gives the capacitance of this element as:

$$dC = \varepsilon_0 \frac{b}{g}\left(1+\frac{2g}{\pi b}\left(1+\ln\left(\frac{\pi b}{g}\right)\right)\right)dx \tag{1}$$

where $g = d_0 - W$ is the gap between capacitor plates. Free charge stored on the capacitor is $\lambda d\hat{x}$, where λ is the free charge per unit length stored on the beam. So the capacitors relation will be of the form:

$$\lambda = \varepsilon_0\left(\frac{b}{d_0-\hat{W}}+\frac{2}{\pi}\left(1+\ln\left(\frac{\pi b}{d_0-\hat{W}}\right)\right)\right)\hat{V} \tag{2}$$

From charge conservation law, the relation between the current along the beam and stored charge is as follows:

$$\frac{\partial \lambda}{\partial \hat{t}} = -\frac{\partial i}{\partial \hat{x}} \tag{3}$$

Ohm's law results:

$$\frac{\partial \hat{V}}{\partial \hat{x}} = -\frac{\hat{\rho}}{bh} i \tag{4}$$

The following equation is obtained by eliminatingλ and i from Eqs. (2), (3) and (4):

$$\frac{\partial^2 \hat{V}}{\partial \hat{x}^2} = \frac{\hat{\rho}\varepsilon_0}{bh}\frac{\partial}{\partial \hat{t}}\left(\left(\frac{b}{d_0-\hat{W}}+\frac{2}{\pi}\left(1+\ln\left(\frac{\pi b}{d_0-\hat{W}}\right)\right)\right)\hat{V}\right) \tag{5}$$

The electrical force per unit length F_e is computed by differentiating with respect to the gap g , the energy per unit length stored inthe capacitor[22], that is:

$$F_e = -\frac{1}{2}V^2\frac{\partial C}{\partial g} \tag{6}$$

Substituting Eq. (1) in Eq. (6) results in:

$$F_e = \frac{b\varepsilon_0 V^2}{2g^2}\left(1+\frac{2}{\pi}\frac{g}{b}\right) \tag{7}$$

The usual Euler-Bernoulli assumption is made so that any plane cross-section, initially perpendicular to the axis of the beam, remains plane and perpendicular to the neutral surface during bending. By incorporatingvonKarman nonlinearityformid-planestretching[22, 23]the differential equation of vibration will be:

$$E_y I_b \frac{\partial^4 \hat{W}}{\partial \hat{x}^4}+\mu\frac{\partial^2 \hat{W}}{\partial \hat{t}^2}-\left(\hat{N}_0+\frac{Ebh}{2l}\int_0^l\left(\frac{\partial \hat{W}}{\partial \hat{x}}\right)^2 d\hat{x}\right)\frac{\partial^2 \hat{W}}{\partial \hat{x}^2} = \frac{1}{2}b\varepsilon_0\frac{\hat{V}^2}{\left(d_0-\hat{W}\right)^2}\left(1+\frac{2}{\pi}\frac{d_0-\hat{W}}{b}\right) \tag{8}$$

where $\hat{N}_0$ is the residual(initial) axial load.

By introducing the following dimensionless parameters:

$$W=\frac{\hat{W}}{d_0}\qquad x=\frac{\hat{x}}{l},\qquad t=\frac{\hat{t}}{T}\qquad T=l^2\sqrt{\frac{\mu}{EI}},\qquad N_0=\frac{\hat{N}_0}{N^*}\qquad N^*=\frac{EI}{l^2}$$
$$V=\frac{\hat{V}}{V^*}\qquad V^*=\frac{d_0}{l^2}\sqrt{\frac{2EId_0}{b\varepsilon_0}},\qquad \rho=\frac{\hat{\rho}}{\rho^*}\qquad \rho^*=\frac{hd_0}{\varepsilon_0}\sqrt{\frac{\mu}{EI}} \tag{9}$$
$$\alpha_1=\frac{bhd_0^{\,2}}{2I}\qquad \alpha_2=\frac{2}{\pi}\frac{d_0}{b}$$

Eqs.(5) and(8) may be non-dimensionalized and the dimensionless coupled nonlinear partial differential equations of motion are derived as:

$$\begin{cases}\dfrac{\partial^4 W}{\partial x^4}+\dfrac{\partial^2 W}{\partial t^2}-\left(N_0+\alpha_1\displaystyle\int_0^1\left(\frac{\partial W}{\partial x}\right)^2dx\right)\frac{\partial^2 W}{\partial x^2}=\frac{V^2}{(1-W)^2}\left(1+\alpha_2(1-W)\right)\\ \dfrac{\partial^2 V}{\partial x^2}=\rho\dfrac{\partial}{\partial t}\left(\left(\dfrac{1}{1-W}+\alpha_2\left(1+\ln\left(\dfrac{2}{\alpha_2}\dfrac{1}{1-W}\right)\right)\right)V\right)\end{cases} \tag{10}$$

The beam deflection and voltage distribution can be written as the sum of two terms as follows:

$$\begin{cases}W(x,t)=W_s(x)+w(x,t)\\ V(x,t)=V_0+v(x,t)\end{cases} \tag{11}$$

Where$W_s(x)$ is the static deflection of the beam and $w(x,t)$ is the amplitude of small vibrations around this static deflection. $V_0$is the constant applied voltage and $v(x,t)$ is the variable term of voltage along the beam.

Substituting Eq. (11) in Eq. (10) and eliminating the terms including time derivatives the governing equation of static deflection is derived as:

$$\frac{d^4W_s}{dx^4}-\left(N_0+\alpha_1\int_0^1\left(\frac{dW_s}{dx}\right)^2dx\right)\frac{d^2W_s}{dx^2}=\frac{V_0^{\,2}}{(1-W_s)^2}\left(1+\alpha_2(1-W_s)\right) \tag{12}$$

Also linearized equations governing the dynamic response around the static deflection will be:

$$\begin{cases}\dfrac{\partial^4 w}{\partial x^4}+\dfrac{\partial^2 w}{\partial t^2}-\left(N_0+\alpha_1\displaystyle\int_0^1\left(\frac{dW_s}{dx}\right)^2dx\right)\frac{\partial^2 w}{\partial x^2}-\left(2\alpha_1\int_0^1\frac{dW_s}{dx}\frac{\partial w}{\partial x}dx\right)\frac{\partial^2 W_s}{\partial x^2}=\\ \dfrac{V_0^{\,2}}{(1-W_s)^3}\left(2+\alpha_2(1-W_s)\right)w+\dfrac{2V_0}{(1-W_s)^2}\left(1+\alpha_2(1-W_s)\right)v\\ \dfrac{\partial^2 v}{\partial x^2}=\rho\left[\dfrac{V_0}{(1-W_s)^2}\left(1+\alpha_2(1-W_s)\right)\dfrac{\partial w}{\partial t}+\left(\dfrac{1}{1-W_s}+\alpha_2\left(1+\ln\left(\dfrac{2}{\alpha_2}\dfrac{1}{1-W_s}\right)\right)\right)\dfrac{\partial v}{\partial t}\right]\end{cases} \tag{13}$$

Using separation of variables the solution may be written as:

$$w(x,t)=\Phi(x)e^{i\omega t}$$
$$v(x,t)=\Psi(x)e^{i\omega t} \tag{14}$$

where $\Phi(x)$ and $\Psi(x)$ are mode shapes for deflection and voltage distribution and ω is the vibration natural frequency. Substituting Eq. (14) into Eq. (13) one obtains:

$$\begin{cases}\Phi^{(4)}-\omega^2\Phi-\left(N_0+\alpha_1\displaystyle\int_0^1\left(\frac{dW_s}{dx}\right)^2dx\right)\Phi''-\left(2\alpha_1\int_0^1\left(\frac{dW_s}{dx}\right)\Phi'dx\right)\frac{d^2W_s}{dx^2} & (a)\\ -\dfrac{V_0^{\,2}}{(1-W_s)^3}\left(2+\alpha_2(1-W_s)\right)\Phi-\dfrac{2V_0}{(1-W_s)^2}\left(1+\alpha_2(1-W)\right)\Psi=0 & (15)\\ \Psi''-i\rho\omega\left[\dfrac{V_0}{(1-W_s)^2}\left(1+\alpha_2(1-W_s)\right)\Phi+\left(\dfrac{1}{1-W_s}+\alpha_2\left(1+\ln\left(\dfrac{2}{\alpha_2}\dfrac{1}{1-W_s}\right)\right)\right)\Psi\right]=0 & (b)\end{cases}$$

In order to solve Eq. (15),W_s as static deflection must be known.

III. Finite element modeling

Finite element method is used to solve Eq. (12). The well-known beam elements which are high order two-node line elements with four degrees of freedom are used. The degrees of freedom are the deflection and slope at each node. Consequently:

$$\Phi = \lfloor N \rfloor \{\phi\} \tag{16}$$

The shape functions are:

$$\lfloor N \rfloor = \lfloor H_{01}^{1} \;\; H_{11}^{1} \;\; H_{02}^{1} \;\; H_{12}^{1} \rfloor \tag{17}$$

Where $H_{mi}^{n}(x)$ are *n*th order Hermite polynomials and m is the order of derivative and i designates either node 1 or node 2. And:

$$\{\phi\} = \begin{Bmatrix} \Phi_1 \\ \Phi_{x1} \\ \Phi_2 \\ \Phi_{x2} \end{Bmatrix} \tag{18}$$

Multiplying the equation by the shape functions and integrating over an element the finite element formulation of the problem for an element is derived:

$$[K]^{(e)} \{\phi\}^{(e)} = \{F\}^{(e)} \tag{19}$$

The stiffness matrix and nodal force vector are:

$$K_{ij} = \int_{\Omega^{(e)}} \left(N_i'' N_j'' + \left(N_0 + \alpha_1 \int_0^1 \left(\frac{dW_s}{dx} \right)^2 dx \right) N_i' N_i' \right) dx \tag{20}$$

$$F_i = \int_{\Omega^{(e)}} \frac{V_0^{\,2}}{(1-W_s)^2} \left[1 + \alpha_2 (1 - W_s) \right] N_i \, dx \tag{21}$$

Where an adaptive Simpson's method with a tolerance of 10^{-8} is used to calculate the integrals.
The boundary conditions of a clamped-clamped beam are:

$$W_s(x) = \frac{dW_s(x)}{dx} = 0 \qquad x = 0,1 \tag{22}$$

Assembling the stiffness matrices and nodal force vectors for all elements and implementing boundary conditions, finite element formulation of the problem is derived.

As can be seen,W_s is appeared in stiffness matrix and nodal force vector. To overcome this problem an iterative method is used to find the solution, starting from zero deflection the force vector and stiffness matrix is calculated and equations are solved and the solution is used for evaluating stiffness matrix and force vector for the next iteration. The iteration is continued until the error is in the range of a predefined tolerance or pull-in occurs. Here we have used a very conservative tolerance of10^{-8}.

After finding the static solution it's time to analyze the free vibration around this deflection. To solve these equations a new electromechanical element which has both Φ and Ψ as field variables, is required to be developed. In the coupled set of governing equations in Eq. (15), the first equation is the equation governing the mechanical beam vibration and the second one governs the electrical voltage distribution. Multiplying these equations bye N_i and integrating with respect to x and implementing part bye part integration, the weak formulation of the governing equations are found in which Φ is appeared up to second order derivatives and Ψ up to first order derivative. Therefore to satisfy compatibility condition in the new element we must have C^1 continuity for variable Φ and C^0 continuity for variable Ψ at element interfaces. Thereforedeflection and its first derivative i.e. slope together with the voltage should be collected as degrees of freedom at each node. So we have:

$$\begin{aligned} \Phi &= \sum_{i=1}^{4} N_i \phi_i \\ \Psi &= N_1 \psi_1 + N_3 \psi_2 \end{aligned} \tag{23}$$

where:

$$\{\phi\}=\begin{Bmatrix}\Phi_1\\ \Phi_{x1}\\ \Phi_2\\ \Phi_{x2}\end{Bmatrix},\qquad \{\psi\}=\begin{Bmatrix}\Psi_1\\ \Psi_2\end{Bmatrix} \tag{24}$$

N_i s which are polynomial shape functions are again same as Eq. (17). Now multiplying the first equation by deflection shape functions and the second one by voltage distribution shape functions and integrating over an element the finite element formulation will be:

$$\left[\begin{array}{c:c}[K_1]_{4\times4} & [K_2]_{4\times2}\\ \hdashline [K_3]_{2\times4} & [K_4]_{2\times2}\end{array}\right]^{(e)}\begin{Bmatrix}\{\phi\}\\ \{\psi\}\end{Bmatrix}^{(e)}=0 \tag{25}$$

where:

$$\begin{aligned}
K_{1_{ij}} &= \int_{\Omega^{(e)}}\left[N_i''N_j''+\left(N_0+\alpha_1\int_0^1\left(\frac{dW_s}{dx}\right)^2dx\right)N_i'N_j'-\left(\omega^2+\frac{{V_0}^2}{(1-W_s)^3}\left(2+\alpha_2(1-W_s)\right)\right)N_iN_j\right]dx\\
K_{2_{ij}} &= \int_{\Omega^{(e)}}\left[-\frac{2V_0}{(1-W_s)^2}\left(1+\alpha_2(1-W)\right)N_iN_j\right]dx\\
K_{3_{ij}} &= \int_{\Omega^{(e)}}\left[i\rho\omega\frac{V_0}{(1-W_s)^2}\left(1+\alpha_2(1-W_s)\right)N_iN_j\right]dx\\
K_{4_{ij}} &= \int_{\Omega^{(e)}}\left[N_i'N_j'+i\rho\omega\left(\frac{1}{1-W_s}+\alpha_2\left(1+\ln\left(\frac{2}{\alpha_2}\frac{1}{1-W_s}\right)\right)\right)N_iN_j\right]dx
\end{aligned} \tag{26}$$

In deriving the preceding equations the term $-\left(2\alpha_1\int_0^1\left(\frac{dW_s}{dx}\right)\Phi'dx\right)\frac{d^2W_s}{dx^2}$ in Eq. (15-a) in which the variable Φ is appeared in the integral and therefore couples the equations of the elements, is neglected. To take into account the effect of this term the following matrix that couples the values of nodal variables at nodes of two different elements must be formed and assembled for every two element k and l as Eq. (27) and to be added to the assembled stiffness matrix derived from the last step, to final stiffness matrix be achieved.

$$K_{k,l}=\left[\begin{array}{c:c}[K']_{4\times4} & [0]_{4\times2}\\ \hdashline [0]_{2\times4} & [0]_{2\times2}\end{array}\right]\qquad k,l=1,2,\ldots,n \tag{27}$$

Where:

$$K'_{ij}=-2\alpha_1\int_{\Omega^{(k)}}\frac{dW_s}{dx}N_i'dx\int_{\Omega^{(l)}}\frac{d^2W_s}{dx^2}N_jdx \tag{28}$$

After finding the stiffness matrix the boundary conditions should be implemented. The boundary condition for deflection Φ is same as Eq. (22). Because the voltage V_0 is applied to the both ends of the beam, according to Eq. (11) the voltage distribution boundary conditions will be:

$$\Psi(x)=0\qquad x=0,1 \tag{29}$$

Finally, the finite element formulation of the problem will be:

$$\left[K(\omega)\right]\begin{Bmatrix}\{\phi\}\\ \{\psi\}\end{Bmatrix}=0 \tag{30}$$

IV. RESULTS AND DISCUSSION

Using the stiffness matrix of Eq. (30) and equating the determinant of the matrix to zero the characteristic equation of the beam frequencies may be found. Then the following procedure is executed to find the natural frequencies. In the first step the complex plane is meshed around the predicted frequency and the characteristic equation is calculated at mesh nodes. At the next step mesh is refined and is constrained around

the nodal mesh pointat which the equation is minimized. This rout is iterated to find the natural frequency with the required precision.

Results show thatthe derived natural frequency fully converges within a precision of $1Hz$ using 20 elements in the model.According to the damping effect of electrical resistivity the derived ωs are complex where the real part is the natural or resonance frequency and the imaginary part is due to damping.

To validate the model, the results are compared with the experimental measured data for micro-beams made of doped silicon with parameters listed in table 1.

Table 1. The parameters of the doubly clamped microbeams[9].

Beam length l (μm)	Width b (μm)	Thickness h (μm)	Initial gap d_0 (μm)	Effective Young's modulus(GPa)	Density γ (kg/m^3)	Residual strain ε_R	Residual axial load N_0 (N)
210 310 410 510	100	1.5	1.18	166	2332	0.0000404	0.000915

The residual axial load is calculated using the residual strain reported in reference [9] by the following relation [9], [12]:

$$N_0 = bhE_y\left(1-\nu^2\right)\varepsilon_R \tag{31}$$

The electrical resistivity is considered to be $\rho = 0.1\Omega m$ the electrical resistivity of phosphorous doped silicon [1].

From Table 2 it is clear that the results of present studypredict the natural frequencies with a smaller deviation from experimental data compared with previous studies reported in this table.

Table 2. A comparison between the experimental measurements and calculated results.

Beam length (μm)	$\omega_0/2\pi(kHz)$								
	[9]			**[12]**		**[14]**		**Present study**	
	Measured	Calculated	error %	Calculated	error %	Calculated	error%	Calculated	error%
210	322.045	324.214	**0.67**	324.70	**0.82**	324.78	**0.85**	322.451	**0.13**
310	163.215	164.347	**0.69**	163.46	**0.15**	163.16	**0.03**	162.355	**0.53**
410	102.169	103.804	**1.60**	103.70	**1.50**	103.42	**1.22**	101.907	**0.26**
510	73.791	74.802	**1.37**	73.46	**0.49**	74.38	**0.80**	73.447	**0.47**

It should be noted that implementing the exact value of the residual axial load plays an important role in the accuracy of the natural frequency and rounding off axial residual force as implemented in previous studies[12]-[14] may result in a better answer while is not legitimately correct.

For systems having one of the following three conditions the effect of electrical resistivity would be significant: 1- systems made of conductors with higher resistivity, 2- systems with smaller size scales, and 3- systems operating at D.C. voltages near the pull-in voltage.

Letthe frequency shift ratio with respect to perfect conductor and damping ratio to be defined as:

$$\Delta\omega = \frac{\mathrm{Re}(\omega)-\omega_0}{\omega_0}$$
$$\xi = \frac{\mathrm{Im}(\omega)}{\omega_0} \tag{32}$$

where ω_0 is the natural frequency at $\rho = 0$.

Fig. 2 shows the frequency shift ratio with respect to dimensionless resistivity. As can be seen in this figure the graph can be divided into three regions in which different effects of electrical resistivity on frequency shift ratio may be distinguished.

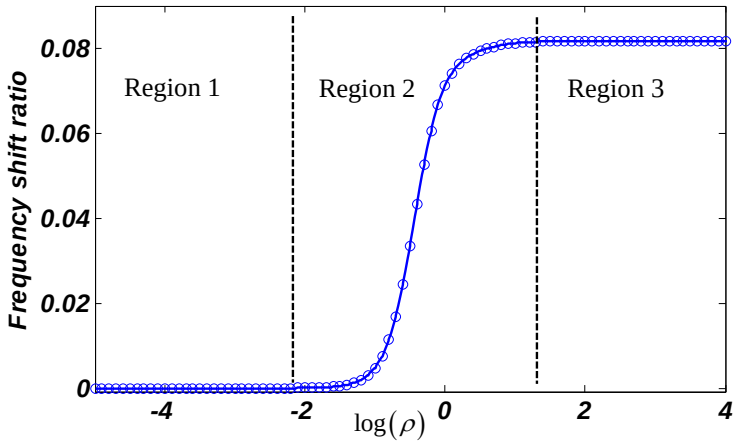

Fig. 2. Effect of electrical resistivity on the frequency shift ratio. ($V_0 = 6,\ \alpha_1 = 3.71,\ \alpha_2 = 0.0075$)

In the first region frequency shift takes place at a very small slope and the system natural frequency is almost the same as the frequency of a perfect conductor beam.

In the second region a jump occurs in frequency shift around a dimensionless resistivity equal to 1. This is due to interaction between mechanical and electrical characteristics of the system. This means when the vibration periodis equal to the RC circuit characteristic time, jump of the frequency shift occurs in the system. In this region, small changes in resistivity cause substantial effect on frequency shift.

In the third region frequency shift ratio is constant. In this region due to the high electrical resistivity of the beam the charge mobility is limited and the charge migration has minimal effect on vibration frequency. In this case voltage enhancement will increase the static deflection and consequently tensile axial stress in the beam which in turn results in increasing of the natural frequency. It is interesting to note that at low resistivities, effect of charge migration lowers the natural frequency and is dominant with respect to mid-plane stretching which tends to enhance the natural frequency.

In region 3, as voltage increases toward pull-in voltage at which the natural frequency of the perfect conductor beam tends toward zero, the frequency shift approaches to infinity.This means as the applied voltage tends toward pull-in voltage;effect of electrical resistivity becomes important and must be considered.

Fig. 3 represents damping ratio versus dimensionless resistivity. This figure can also be divided into three regions where in regions 1 and 3 damping ratio is negligible while in region 2 damping ratio shows a substantial jump around dimensionless resistivity of 1. The maximum of this jump takes place at a specific resistivity which is called critical resistivity ρ_{cr} , hereinafter.

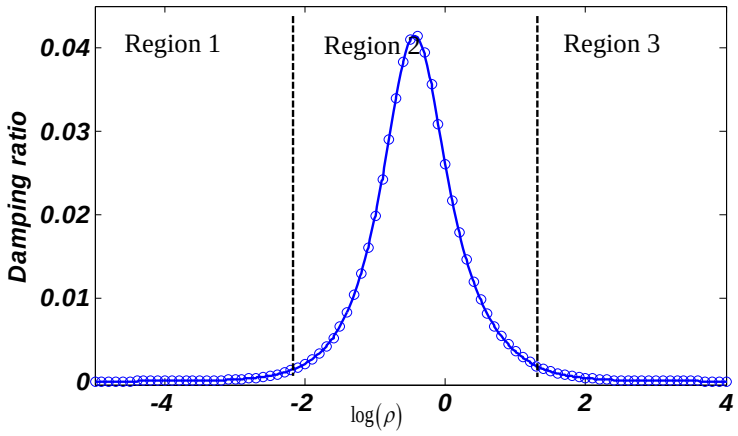

Fig. 3. Effect of electrical resistivity on the damping ratio. ($V_0 = 6,\ \alpha_1 = 3.71,\ \alpha_2 = 0.0075$)

To have a quantitative analysis and to clarify the key role of electrical resistivity in design of micro and Nano structures and the effect of size scale, two special cases are considered. The first case is a micro resonator where a doubly clamped micro-beamis surrounded by a vacuum atmosphere and the second case is a Nano resonator made of a doubly clamped nano-bridge immersed in water with relative permittivity of $\varepsilon_r =$ 80(neglecting dielectric elasticity)[25, 26].

The beams are actuated by a D.C. voltage that is applied to theirboth clamped ends. Assuming that the beams are made of silicon, their physical properties including Young's modulus and density are same as table 2. The

geometrical properties are given in table 3, andthe critical resistivities for these two cases are reported in the same table.

Electrical resistivity of undoped silicon is 10^3 and by doping process can be changed between 10^3 and 10^{-4} with respect to the portion of impurity. According to Table 1 and Figs. 2 and 3, the jump region in case 1 completely falls in this interval. Therefore for a microbeam made of silicon, impurity portion may be adjusted to achieve the proper electrical resistivity and meet desired frequency shift and damping ratios. When no damping is desirable, impurity can be adjusted so that the electrical resistivity becomes very smaller than this critical resistivity.While for a nanobeam, even with fully doped silicon damping occurs and when damping is undesired in the designed device the selected material should be a better conductor.

Table 3. Critical resistivity the micro and nano beam.

Case	Length (l)	Initial gap (d_0)	Critical resistivity (ρ_{cr})
1	$200\mu m$	$1\mu m$	$20.5\Omega.m$
2	$1\mu m$	$25nm$	$0.0064\Omega.m$

V. CONCLUSIONS

Vibration characteristics including resonance frequency and damping of electrostatically actuated micro and nano resonators made of non-perfect conductor materials are investigated. Governing coupled nonlinear partial differential equations of deflection and voltage distribution are developed and a new electromechanical element is designed to be implemented in the formulation. Comparison of the calculated resonance frequencies with the measured data shows very good agreement. Results indicate that electrical resistivity effect causes a jump in frequency and damping of the system and frequency shift tends asymptotically to a constant value as the resistivity increases while the damping ratio tends toward zero. The maximum amplitude of the jump enhances as the applied voltage approaches toward pull-in voltage and the critical resistivity at which jump occurs takes place at lower resistivities as the size of the structure decreases from micro to nano scale.

REFERENCES

[1] R. Legtenberg, H.A. Tilmans, "Electrostatically Driven Vacuum-Encapsulated Polysilicon Resonators Part I. Design And Fabrication,"Sensors And Actuators A: Physical, 45 (1994) 57-66.

[2] W.H. Ko, Q. Wang, "Touch Mode Capacitive Pressure Sensors," Sensors And Actuators A: Physical, 75 (1999) 242-251.

[3] A.A. Seshia, M. Palaniapan, T.A. Roessig, R.T. Howe, R.W. Gooch, T.R. Schimert, S. Montague, "A Vacuum Packaged Surface Micromachined Resonant Accelerometer,"Journal Of Microelectromechanical Systems, 11 (2002) 784-793.

[4] J.-M. Huang, K. Liew, C. Wong, S. Rajendran, M. Tan, A. Liu, "Mechanical Design And Optimization Of Capacitive Micromachined Switch", Sensors And Actuators A: Physical, 93 (2001) 273-285.

[5] Z. Olszewski, M. Hill, C. O'mahony, R. Duane, R. Houlihan, "Characterization, Modelling And Performance Evaluation Of Cmos Integrated Multielectrode Tunable Capacitor (Mtc)", Journal Of Micromechanics And Microengineering, 15 (2005) S122.

[6] P.M. Osterberg, S.D. Senturia, "M-Test: A Test Chip For Mems Material Property Measurement Using Electrostatically Actuated Test Structures, Journal Of Microelectromechanical Systems, 6 (1997) 107-118.

[7] P. Kim, C.M. Lieber, Nanotube Nanotweezers, Science, 286 (1999) 2148-2150.

[8] D.J. Ijntema, H.A. Tilmans, "Static And Dynamic Aspects Of An Air-Gap Capacitor", Sensors And Actuators A: Physical, 35 (1992) 121-128.

[9] H.A. Tilmans, R. Legtenberg, "Electrostatically Driven Vacuum-Encapsulated Polysilicon Resonators," Part Ii. Theory And Performance, Sensors And Actuators A: Physical, 45 (1994) 67-84.

[10] M. Moghimi Zand, M. Ahmadian, "Characterization Of Coupled-Domain Multi-Layer Microplates In Pull-In Phenomenon," Vibrations And Dynamics, International Journal Of Mechanical Sciences, 49 (2007) 1226-1237.

[11] M. Moghimi Zand, M. Ahmadian, "Vibrational Analysis Of Electrostatically Actuated Microstructures Considering Nonlinear Effects," Communications In Nonlinear Science And Numerical Simulations, 14 (2009) 1664-1678.

[12] J.-H. Kuang, C.-J. Chen, "Dynamic Characteristics Of Shaped Micro-Actuators Solved Using The Differential Quadrature Method," Journal Of Micromechanics And Microengineering, 14 (2004) 647.

[13] E.-R. König, G. Wachutka, "Multi-Parameter Homotopy For The Numerical Analysis Of Mems," Sensors And Actuators A: Physical, 110 (2004) 39-51.

[14] M. Moghimi Zand, M. Ahmadian, B. Rashidian, "Semi-Analytic Solutions To Nonlinear Vibrations Of Microbeams Under Suddenly Applied Voltages," Journal of Sound And Vibration, 325 (2009) 382-396.

[15] M.I. Younis, "Modeling And Simulation Of Microelectromechanical Systems In Multi-Physics Fields," InCiteseer, 2004.

[16] A.H. Nayfeh, M.I. Younis, "A New Approach To The Modeling And Simulation Of Flexible Microstructures Under The Effect Of Squeeze-Film Damping," Journal Of Micromechanics And Microengineering, 14 (2003) 170.
[17] R.C. Batra, M. Porfiri, D. Spinello, "Effects Of Van Der Waals Force And Thermal Stresses On Pull-In Instability Of Clamped Rectangular Microplates," Sensors, 8 (2008) 1048-1069.
[18] R. Batra, M. Porfiri, D. Spinello, "Effects Of Casimir Force On Pull-In Instability In Micromembranes," Epl (Europhysics Letters), 77 (2007) 20010.
[19] R. Batra, M. Porfiri, D. Spinello, "Reduced-Order Models For Microelectromechanical Rectangular And Circular Plates Incorporating The Casimir Force," International Journal Of Solids And Structures, 45 (2008) 3558-3583.
[20] W.-H. Lin, Y.-P. Zhao, "Nonlinear Behavior For Nanoscale Electrostatic Actuators With Casimir Force," Chaos, Solitons & Fractals, 23 (2005) 1777-1785.
[21] A. Ramezani, A. Alasty, J. Akbari, "Pull-In Parameters Of Cantilever Type Nanomechanical Switches In Presence Of Casimir Force," Nonlinear Analysis: Hybrid Systems, 1 (2007) 364-382.
[22] R. Batra, M. Porfiri, D. Spinello, "Vibrations Of Narrow Microbeams Predeformed By An Electric Field," Journal Of Sound And Vibration, 309 (2008) 600-612.
[23] E.M. Abdel-Rahman, M.I. Younis, A.H. Nayfeh, "Characterization Of The Mechanical Behavior Of An Electrically Actuated Microbeam," Journal Of Micromechanics And Microengineering, 12 (2002) 759.
[24] H.B. Palmer, "The Capacitance Of A Parallel-Plate Capacitor By The Schwartz-Christoffel Transformation," American Institute Of Electrical Engineers, Transactions Of The, 56 (1937) 363-366.
[25] C. Chen, M. Ma, J. Zhe Liu, Q. Zheng, Z. Xu, "Viscous Damping Of Nanobeam Resonators," Humidity, Thermal Noise, And A Paddling Effect, Journal Of Applied Physics, 110 (2011) 034320-034320-034325.
[26] P. Bøggild, T.M. Hansen, C. Tanasa, F. Grey, "Fabrication And Actuation Of Customized Nanotweezers With A 25 Nm Gap," Nanotechnology, 12 (2001) 331.